

STUDY ON NATURAL VIBRATION AND NONLINEAR SEISMIC RESPONSE OF CONCRETE FILLED TUBULAR (CFT) ARCH BRIDGE CONSTRUCTED IN CHINA

Q. Wu^{*}, B. Chen[†], K. Takahashi^{*}, H. Matsuzaka^{*} and S. Nakamura^{*}

^{*} Department of Civil Engineering, Faculty of Engineering
Nagasaki University
1-14, Bunkyo-machi, Nagasaki, Japan
e-mail: takahasi@civil.nagasaki-u.ac.jp

[†] College of Civil Engineering and Architecture
Fuzhou University
523# Gong ye Road, Fuzhou, China
e-mail: baochunchen@fzu.edu.cn

Key words: Concrete filled steel tube, arch bridge, nonlinear seismic response, lateral bracing

Abstract. *CFT structures are a rational design choice for the arch ribs of an arch bridge since CFT is resistant to axial compressive forces. Japan's first CFT arch highway bridge, the Second Saikai Bridge, is now under construction. Civil engineering structures must be seismically safe. Therefore, the seismic safety of CFT arch bridges under strong earthquakes must be confirmed. This paper analyzes a CFT bridge in China that has the same span with the Second Saikai Bridge. The natural vibration characteristics of this bridge are discussed using a three-dimensional FE model. A nonlinear seismic analysis is performed using the strong ground motions observed in the Hyogo-ken Nanbu Earthquake in Japan, and the properties of this bridge's nonlinear seismic vibration are discussed. The results verify the fine performance of this CFT bridge under strong seismic motions. Furthermore, since the arrangement of the lateral bracings can be considered a countermeasure for the out-of-plane seismic responses of the arch bridge, this paper examines the effect of lateral bracing on the nonlinear seismic response of an arch rib and concluded that lateral bracings in the quarter span of the CFT bridge may greatly reduce seismic vibrations.*

1 INTRODUCTION

Using concrete filled steel tubes (CFT) for the arch ribs of an arch bridge is rational since CFT is resistant to axial compressive forces. The infilled concrete delays local buckling of the steel tube and the steel tube reinforces the concrete's resistance to tension, bending moments, and shear forces^{i, ii}. The tube also acts as a formwork for the concrete during construction of the bridge, thus eliminating a major construction costⁱⁱⁱ. Because of these advantages, it is possible to reduce the cost of constructing steel bridges^{iv, v}. In Japan, CFT arch bridges have recently been the subject of research analysis and experiments. The Second Saikai Bridge, which is under construction in Nagasaki Prefecture, is the first CFT arch highway bridge in Japan^{vi}.

More than 100 CFT arch bridges have been constructed in China since the 1990's and those constructed recently are greatly improved. For example, the tubes of the arch ribs are only partially filled with concrete, and horizontal steel beams instead of horizontal RC beams are to decrease vehicle-induced vibrations in the girder. These technological studies have led to the current construction of a CFT arch bridge with a span of 460m^{vii}.

The CFT arch bridge may be a rational choice in China, where there is only a slight possibility of strong earthquakes occurring. In Japan, the seismic safety of CFT arch bridges must be verified. Since the Hyogo-ken Nanbu Earthquake, bridges must be ductile^{viii}. Since a CFT arch rib is heavier than a steel rib and the arch action is not effective in the out-of-plane direction, the effect of a large earthquake force in the out-of-plane direction on CFT arch bridges is a concern.

Liu et al. clarified the nonlinear seismic performance of the tentatively designed CFT arch bridges according to the Japan design standard after discussing the seismic characteristics of two CFT arch bridges in China^{ix}. Wu et al. discussed the nonlinear seismic properties of a partially concrete filled steel tubular arch bridge in China and examined the effect of the filled concrete length of steel tube on the nonlinear seismic response of an arch bridge^x. More studies are necessary in order to fully comprehend the seismic properties of CFT arch bridges.

In this paper, the authors analyze a CFT bridge in China in an attempt to evaluate the dynamic characteristics of the CFT arch bridge in terms of their response to strong seismic excitations. A CFT bridge in China is made to be the analysis object. This bridge has three spans. The main span of the half-through CFT arch bridge has a span of 251m, which is similar to the length of the Second Saikai Bridge, Japan's first CFT arch highway bridge.

This paper begins by describing the three-dimensional finite element model that was used in the experiment and discussing the natural vibration characteristics of this bridge. A nonlinear seismic analysis is then performed using the strong ground motions recommended in the Design Specification for Highway Bridges 1996^{viii}. Axial force fluctuation and the non-linearity of the biaxial bending moments of the CFT arch rib are taken into account by using a fiber model. The results verify the fine performance of this bridge under strong ground motions.

This paper also examines the effect of the arrangement of the lateral bracings on the seismic vibration of the arch rib.

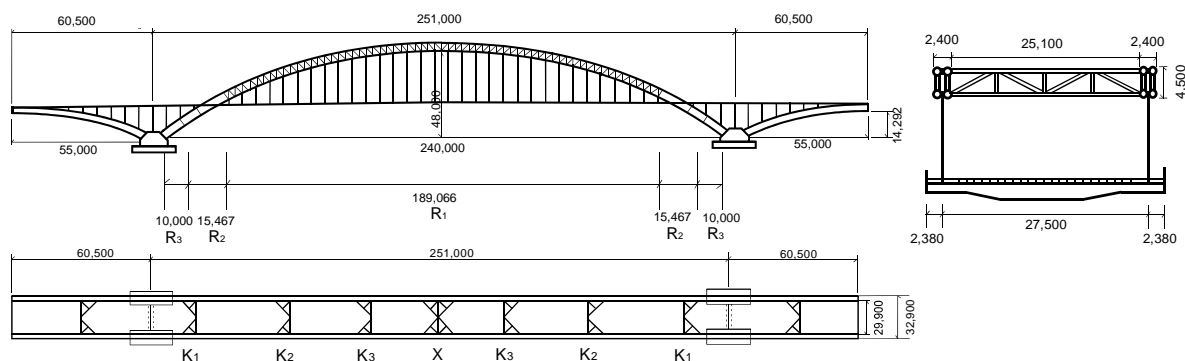


Figure 1 General characteristics of CFT bridge (unit: mm)

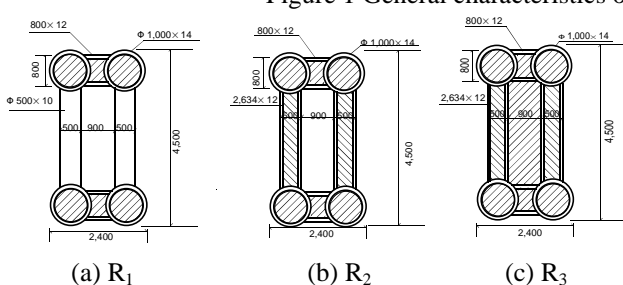


Figure 2 Section of arch rib (unit: mm)

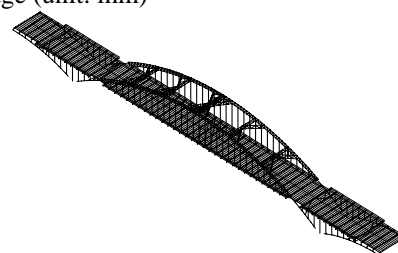


Figure 3 FE model

2 BRIEF DESCRIPTION

The object of this analysis is an arch bridge with three spans that was constructed in China. As shown in Figure 1, this bridge is a rigid-frame tied bridge with spans of 60.5 m, 251 m and 60.5 m. The main span is a half-through CFT arch bridge. The side spans are two cantilevered half RC arch bridges. Because this bridge is self-balancing, prestressed steel ties are used to balance the horizontal force in the piers. The half-through CFT arch bridge has a 240.0m clear span and a 48.0m clear rise, and the upper-deck RC arch bridges have 55.0 m clear spans and 14.3 m clear rises.

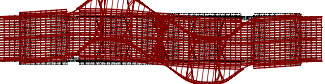
The CFT arch rib has three cross sections (R_1 , R_2 and R_3), as shown as Figure 2. Each of the three cross sections is composed of two horizontal dumbbells. Each dumbbell is comprised of two steel tubes and two plates with a concrete filled inner space. The diameter of the steel tube is 1000 mm and the thickness is 14mm. The steel plate is 800×12mm. The three cross sections differ in the type of connection between the two horizontal dumbbells. The R_1 member in the center part of the main span is connected by vertical and diagonal truss tubes. The R_2 member is near the joint between the arch rib and the floor system, and the two horizontal dumbbells are connected with web steel plates instead of steel tubes. The inner spaces of the web bars are filled with concrete. The R_3 member is in the region start from springing part and ending at a horizontal distance of 10 meters. The R_3 cross section contains infilled concrete not only in the inner span of the web but also in the core of the cross section. The reason for filling the inner space with concrete is to prevent collapse should the bridge suffer a collision with a ship, since the maximum water depth of the river is about 7-8 meters away from the springing part of the arch rib.

Six K-type lateral bracings, one X-type lateral bracing in the arch rib of the main span, and

Table 1 Natural modes of in-plane vibrations

No.	Freq. (Hz)	Participation factor		
		X dir.	Y dir.	Z dir.
2	0.724	37.2588	0.0000	-0.0805
				
6	1.229	0.0000	23.0828	0.0000
				

Table 2 Natural modes of out-of-plane vibrations

No.	Freq. (Hz)	Participation factor		
		X dir.	Y dir.	Z dir.
1	0.385	-0.0007	0.0000	83.7519
				
3	0.760	0.0000	0.4989	0.0000
				

two K-type lateral bracings in the arch ribs of the side spans are used to ensure the out-of-plane stability of the arch ribs.

Instead of concrete horizontal beams, steel horizontal beams are used for decreasing vehicle-induced vibrations in the girder. The main girders are T-type RC beams.

3 MODEL USED IN ANALYSIS

Figure 5 is a three-dimensional finite element model of this bridge. Regarding the modeling of the arch rib, the R_1 member is modeled using two beam elements, which represent the upper and lower horizontal dumbbells, respectively. Truss elements are used to model the vertical and diagonal truss tubes. The R_3 and R_2 members, which have concrete filled inner spaces, are considered to be a single member and are modeled using single beam elements. The single tie is replaced by two spring elements with equivalent rigidity; these two spring elements are positioned at the two ends of the deck.

The following boundary conditions are assumed in this model: (i) all displacements at the end supports of the arch rib are fixed; (ii) the longitudinal displacement, as well as the rotation around the longitudinal direction, are free at the end supports of the deck, while the other freedoms of the deck are constrained.

4 NATURAL VIBRATION PROPERTIES

The lowest natural frequencies and the corresponding participation factors and modal shapes are shown in Tables 1 and 2.

The first in-plane vibration is the antisymmetric mode and has a frequency of 0.724 Hz. The second in-plane vibration has a frequency of 1.229 Hz, which corresponds to the symmetric mode of the arch rib.

The first out-of-plane vibration is the symmetric mode and has a frequency of 0.385 Hz, which is lower than the frequency of the first in-plane mode.

5 SEISMIC RESPONSE PROPERTIES

5.1 Analytical conditions and earthquake loadings

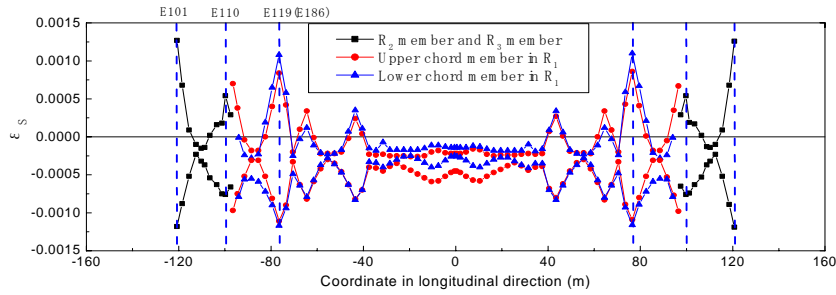


Figure 4 Maximum strains at the extreme edge of steel tubes

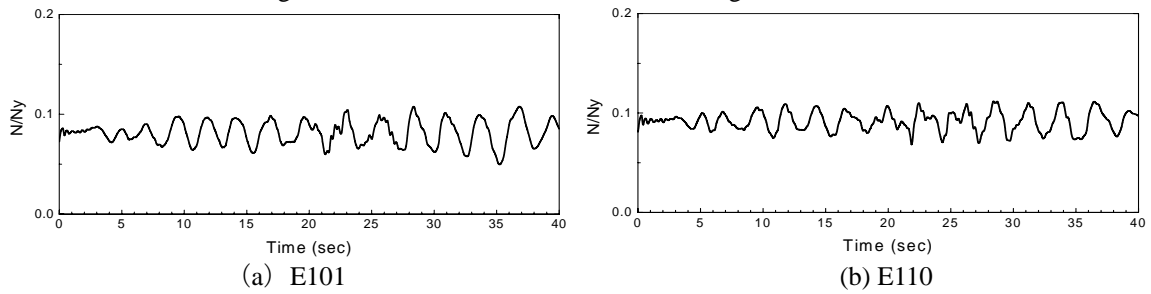
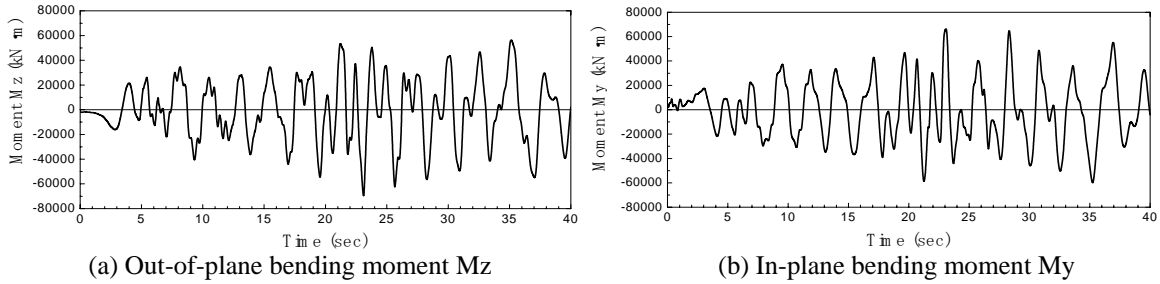
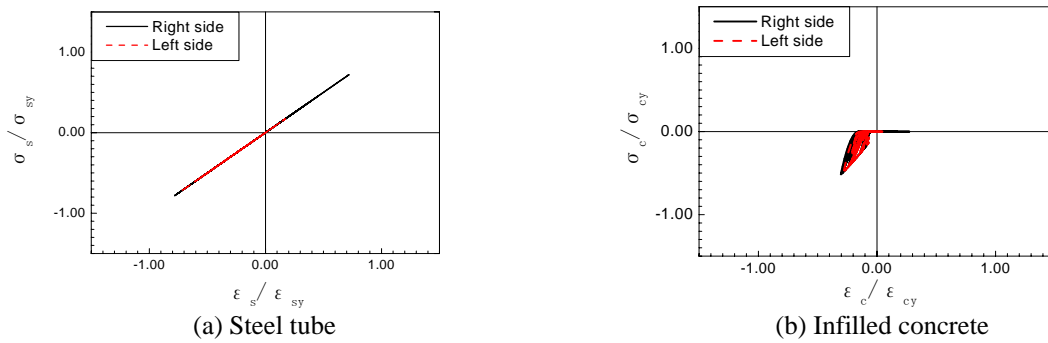


Figure 5 Time history of axial force



(a) Out-of-plane bending moment M_z (b) In-plane bending moment M_y

Figure 6 Time history of bending moments in element E101



(a) Steel tube (b) Infilled concrete

Figure 7 Stress-strain curves of steel tube and infilled concrete

In order to consider the material non-linearity used for the CFT arch ribs, a fiber model is used. This model can automatically take into account axial force fluctuation and the non-linearity of the biaxial bending moments. An elastic perfect plastic model of the steel tube is used. The stress-strain curve proposed by Sato^{xi}, which takes into account the confinement of the infilled concrete, is used to determine the material non-linearity of the concrete inside the steel tube. The yield stress and yield strain are calculated using the following equations:

$$\text{Yield stress } f_{cB} = -\{\sigma_{ck} + 0.8(2t/D)\sigma_{sy}\} \quad (1)$$

$$\text{Yield strain } \varepsilon_{cB} = -(2.5 + 0.025\sigma_{ck}) \times 10^{-3} (\sigma_{ck} : \text{N/mm}^2) \quad (2)$$

where, σ_{sy} is the yield stress of the steel tube, σ_{ck} is the specified concrete strength, t is the thickness of the steel tube, and D is the outer diameter of the steel tube.

Because the properties of the concrete inner plates are not equivalent to the inner spaces of the steel tubes, the hoop action of the concrete in the steel tube is not considered in the analysis of the concrete inner plates.

Nonlinear dynamic analysis is performed using the Newmark β method ($\beta=1/4$) of direct integration. The time interval of the numerical integration is 1/400 sec. Rayleigh damping is employed and the damping coefficients of all members are assumed to 0.02. Two of the modes used for Rayleigh damping are the first and second out-of-plane modes.

The ground motions used in this analysis are based on the Design Specification for Highway Bridges in Japan^{viii}. They are standard strong earthquakes of Type I (T111, T112, T113) in conditions of stiff soil. The initial stress on the bridge is assumed to be the stress that is present under the dead-load condition.

5.2 Characteristics of actual bridge subjected to out-of-plane ground motions

When the bridge is subjected to a T113 earthquake in the out-of-plane direction, the maximum strains at the extreme edges of the steel tubes are as shown in Figure 4. The ordinate is the strains on the steel tube and the abscissa is the coordinates in the longitudinal direction of the bridge. Element E101 of the R_3 member in the springing part generates the maximum strain. The maximum strain of the R_2 member is generated in E110 near the joint between the arch rib and the floor system. For the R_1 member, the largest strain is generated near lateral bracing K_2 of the arch rib (the upper chord member E119 and the lower chord member E186). The strains in the lower chord members are larger than those in the upper chord members.

Time histories of the axial forces N are shown in Figure 5. Because the axial forces of the arch rib are essentially compressive forces, the yield compressive force N_y is used and the non-dimensional axial force N/N_y is shown along the vertical axis of the figure. Fluctuations in the axial forces are small since the maximum values are less than 10% of their yield compressive forces.

Time histories of the out-of-plane bending moment M_z and the in-plane bending moment M_y are shown in Figure 6. It is known that very large amounts of in-plane bending moment M_y of the arch rib are generated in addition to the out-of-plane bending moment M_z , even when

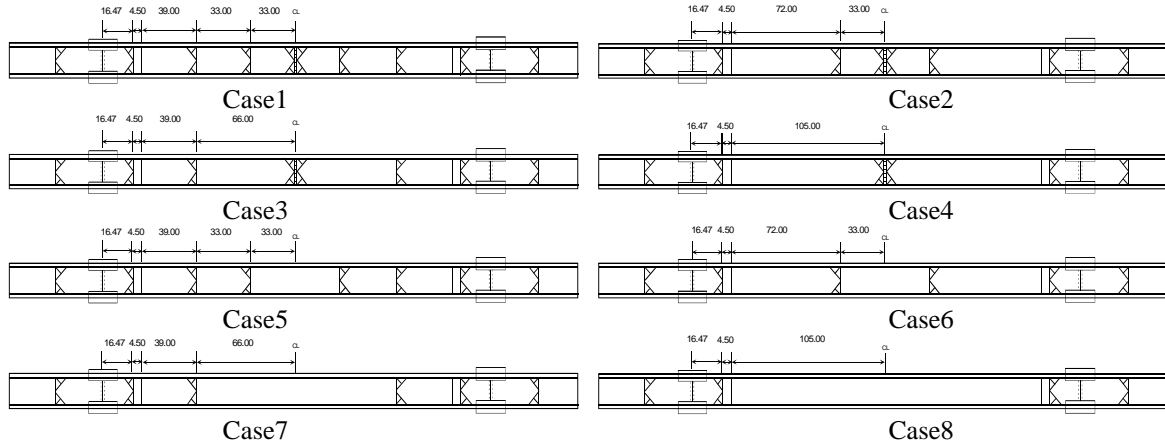


Figure 8 Analytical cases

the ground motion is applied in the out-of-plane direction. Because the in-plane and out-of-plane bending moments are generated simultaneously, the analysis must consider the biaxial bending moment of the arch rib.

Figure 7 shows the stress-strain curves of the steel tube and the infilled concrete at the extreme edge. The vertical axis corresponds to the ratio of the stress (σ_s , σ_c) to the absolute value of the yield stress (σ_{sy} , f_{cB}), and the longitudinal axis corresponds to the ratio of the strain (ε_s , ε_c) to the absolute value of the yield strain (ε_{sy} , ε_{cB}). The maximum strains in both the steel tubes and the infilled concrete do not reach the yield strain. Therefore, the arch rib of this CFT arch bridge is not damaged.

6 EFFECT OF ARRANGEMENT OF LATERAL BRACINGS ON RESPONSES OF CFT ARCH RIBS

6.1 Analytical cases

For our study, we rearrange the X-type, K_2 -type and K_3 -type lateral bracings for the arch rib in the main span. Figure 8 shows the eight analytical models used in this paper. Case 1 corresponds to the actual bridge. Cases 2 through 4 are different combinations that have X-type lateral bracings. Cases 5 through 7 are combinations without X-type lateral bracings. Case 8 corresponds to a model without those lateral bracings.

6.2 Effect of arrangement of lateral bracings on natural vibrations

In Figure 9, the natural frequencies of the out-of-plane modes are sorted according to the modal shapes of Case 1 (actual bridge, see Table 2). The arrangement of lateral bracings has such a small effect on the in-plane natural modes that this paper does not discuss in-plane modes.

Figure 9(a) shows the first and second natural frequencies of the out-of-plane symmetrical modes. Comparing Cases 1, 3, 5 and 7, which have K_2 lateral bracings, with Cases 2, 4, 6 and 8, which do not have K_2 lateral bracings, the structure with K_2 lateral bracings has higher natural frequencies than the structure without K_2 lateral bracings. The effect of the X-type lateral bracing on the out-of-plane symmetrical modes is small because the frequencies of

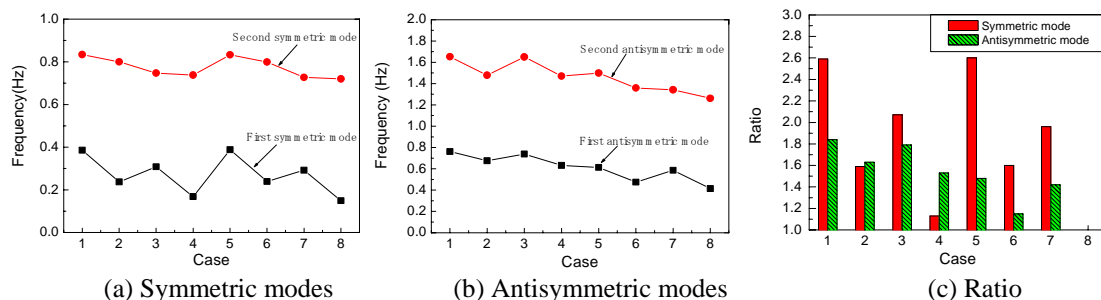


Figure 9 Natural frequencies of out-of-plane modes

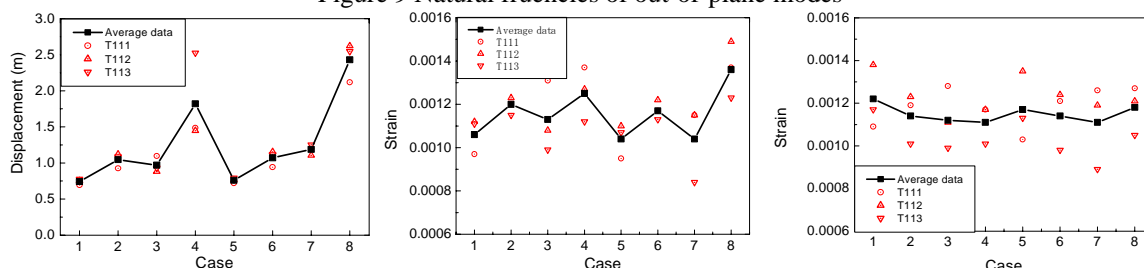


Figure 10 Out-of-plane displacement

Figure 11 Strains of steel tube in R_1 member

Case 5, which does not have X-type lateral bracing, is almost same as that of Case 1, which does. Therefore, K_2 lateral bracings have a large effect on the first out-of-plane symmetrical mode, while the X-type lateral bracing has a small effect on the first out-of-plane symmetrical mode.

The ratio between the frequencies of each case and those of Case 8, in which there aren't X-type lateral bracing, K_2 -type and K_3 -type lateral bracings, is shown in Figure 9(c). The natural frequencies of the first out-of-plane symmetric modes are higher than those of Case 8, which does not have lateral bracings. The natural frequencies of Cases 1 and 5, which have K_2 -type and K_3 -type lateral bracings, is 160% greater than that of Case 8, which does not have lateral bracings.

Figure 9(b) shows the first and second natural frequencies of the out-of-plane antisymmetric modes. X-type lateral bracing has an effect on the out-of-plane antisymmetric modes in all cases. Figure 9(c) shows that the first frequencies of the out-of-plane antisymmetric modes in Cases 1 and 3, which have X-type lateral bracing, are 80% greater than that of Case 8, which does not have lateral bracings.

6.3 Effect of arrangement of lateral bracings on seismic responses of arch ribs

The effect of the arrangement of the lateral bracings on the seismic responses of arch ribs is also examined. In this case, the bridge is subjected to earthquake excitations in the out-of-plane direction. In general, the characteristics of the ground motions greatly influence a bridge's response. Even when the ground motions have the same response spectrum, the bridge can have different responses. To solve this problem, this paper uses the mean value of the maximum responses for three strong ground motions, as recommended in Design Specifications for Highway Bridges in Japan^{viii}. The ground motions used in this analysis are the standard ground motions T111, T112 and T113.

Figures 10 and 11 show the mean values of the maximum out-of-plane displacements in the crown part of arch ribs, and the maximum strains on the R_1 member, respectively.

Figure 10 shows that the out-of-plane displacements in Case 1, which has X-type lateral bracing, and in Case 5, which does not, are smaller than the displacements in the other cases. Therefore, the use of the K_2 -type and K_3 -type lateral bracings can decrease the seismic displacements of arch ribs.

The effect of X-type lateral bracing on the seismic displacements of arch rib isn't great since the out-of-plane displacements in Cases 1 and 5 are of the same order.

Figure 11 shows that, the change in the maximum strains generated in the upper chord members is greater than that in the lower chord members. The maximum strains in the upper chord members in Cases 1, 3, 5, and 7, which have K_2 -type lateral bracing, are smaller than those in the other cases. Therefore, K_2 -type lateral bracing can decrease the seismic responses of arch ribs.

The ratios of the responses between each case and Case 8 are shown in Figure 12. The out-of-plane displacements and the strains of the upper chord member in Case 5, which have K_2 -type and K_3 -type lateral bracings, are about 30% and 20% less than those in Case 8, which does not have lateral bracings. Therefore, placing some lateral bracings near the quarter span of arch ribs seems to effectively decrease the seismic responses of this CFT arch bridge when it is subjected to a uniform out-of-plane earthquake.

7 CONCLUSIONS

This paper evaluated the seismic response characteristics of a CFT arch bridge and the effect of the arrangement of lateral bracings on the seismic vibrations of the arch rib.

The main findings on the properties of a CFT arch bridge are as follows:

- The antisymmetric mode is the first in-plane vibration, and the symmetric mode is the first out-of-plane vibration.
- Biaxial bending moments should be considered in the seismic analysis of a CFT arch rib, because in-plane and out-of-plane bending moments are generated simultaneously when the bridge is subjected to an earthquake in the out-of-plane direction.
- The fine performance of this CFT bridge is confirmed because the strains in arch ribs do not reach the yield strains.

What is worrying about CFT arch bridges is the increase in the out-of-plane responses of arch ribs when subjected to an out-of-plane ground motion. Placing some lateral bracings near the quarter span of arch ribs decreases the responses of the CFT arch ribs. The arrangement of lateral bracings has the following effects.

- The natural frequencies of the out-of-plane symmetric modes for cases that have K -type lateral bracings near the quarter span of arch ribs is 160% larger than that those for cases that do not have lateral bracings.
- The natural frequencies of the out-of-plane antisymmetric modes for cases that have

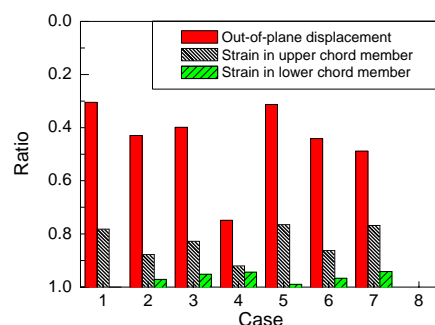


Figure 12 Ratio of maximum responses

X-type lateral bracings in the half span of arch rib are 80% larger than those for cases that do not have lateral bracings.

- The out-of-plane displacements and the strains in the upper chord members that have K-type lateral bracings near the quarter span of arch ribs are about 30% and 20% less than those in the upper chord members that do not have lateral bracings.

REFERENCES

- [i] C.W. Roeder, B. Cameron and C.B. Brown, Composite action in concrete filled tubes, *Journal of Structural Engineering*, ASCE, Vol.125, No.5, 477-484 (1999)
- [ii] A.H. Varma, J.M. Ricles, R. Sause and L.W. Lu, Experimental behavior of high strength square concrete-filled steel tube beam-columns, *Journal of Structural Engineering*, ASCE, Vol.128, No.3, 309-318 (2002)
- [iii] Z. Zhen, B. Chen and Q. Wu, Recent Development of CFST Arch Bridge in China, *Proceeding of 6th ASCCS Conference*, pp.205-212 (2000)
- [iv] W.C. Clawson, *Bridge Applications of Composite Construction in the U.S.*, *Structural Engineering in the 21st Century*, *Proceedings of the 1999 Structures Congress*, 544-547, (1999)
- [v] S. Nakamura, New structural forms for steel/concrete composite bridges, *Structural Engineering International 1*, *Journal of the International Association for Bridge and Structural Engineering (IABSE)*, 45-50 (2000)
- [vi] Q. Wu, B. Chen, K. Takahashi and S. Nakamura, Construction and technical subjects of concrete filled steel tubular arch bridges in China, *Bridge and Foundation Engineering*, Vol.35, No.10, 40-45 (2001) (in Japanese)
- [vii] D. Peng, Q. Wu, K. Takahashi and S. Nakamura, Recent construction and development of long-span bridges in China, *Bridge and Foundation Engineering*, Vol.37, No.2, 43-49 (2003) (in Japanese)
- [viii] Japan Road Association, *Design Specifications for Highway Bridges, Part V: Seismic Design* (1996) (in Japanese)
- [ix] Y. Liu and H. Hikosaka, Assessment for ultimate strength and seismic performance of braced-rib arch bridge using concrete-filled tubes, *Journal of Structure Mechanics and Earthquake Engineering*, JSCE, No.703/I-59, 313-325 (2002) (in Japanese)
- [x] Q. Wu, K. Takahashi, H. Matsuzaka, B. Chen and S. Nakamura, Study on dynamic properties of partially concrete filled steel tubular arch bridge, *Journal of Constructional Steel*, Vol.10, 141-148 (2002) (in Japanese)
- [xi] T. Sato, Confining mechanism and analytical model in circular concrete-filled steel tube under axial force, *Journal of Structure Construction Engineering*, AIJ, No.452, 149-158 (1993) (in Japanese)